

The Sea of Okhotsk Geotraverse: Tectonomagmatic Evolution of Cenozoic Extension Structures and Implication for Their Deep Structure

N. I. Filatova^a and A. G. Rodnikov^b

Presented by Academician V.E. Khain, January 30, 2006

Received February 1, 2006

DOI: 10.1134/S1028334X06090030

Issues of the origin of marginal seas and genesis of their igneous rocks remain controversial because of the insufficient amount of documentary information (small number of drilled holes, rare network of seismic profiles, and so on). Therefore, data on seismic profiles carried out within the framework of the Geotraverse International Project [1, 2] are of great significance. The geotraverse extends from the margin of Asia (Sikhote Alin) to the northwestern periphery of the Pacific plate (Fig. 1) and includes large Cenozoic extension structures, such as the Tatar continental rift and the South Kuril marginal basin. Comprehensive analysis of seismic data on deep zones of this profile coupled with the available information about the regional tectonic setting and magmatism have made it possible to detect a correlation between the Cenozoic geodynamic mode (correspondingly, tectonics and magmatism) at the crustal and deeper (lithospheric mantle and asthenosphere) levels. Ultimately, these data made it possible to refine the evolution model of marginal basins in the study region and provided new insights into the issue of passive and active rifting.

The *Tatar continental rift* located in the western part of the geotraverse (Fig. 2) represents the northern termination of the Japan basin. Both structures are bounded by a convergent system of submeridional dextral strike-slip faults partly transformed into normal faults. The Tatar rift basement incorporates a thin continental crust with the velocity of seismic waves (hereafter, V) ranging from 5.8 to 7.2 km/s [4, 7]. The continental crust began to break down after its disintegration in the terminal Paleocene–Eocene into a system of nar-

row (5–10 km) horsts and grabens [2, 4] and the accumulation of terrigenous sediments (up to 1.5 km thick) at the initial rifting stage. The next (Oligocene–middle Miocene) stage of maximum extension of the Tatar rift is marked by the unconformably overlying transgressive sequence of deep-water clayey and siliceous–clayey rocks (up to 4 km). The next (middle Miocene) regressive sequence is composed of coastal-marine sediments. In contrast to the almost undeformed cover of middle Miocene–Holocene terrigenous rocks (1.5–5 km thick) deposited after the rifting (hereafter, postrift complex), rocks deposited during rifting (rift complex) are characterized by significant dislocations. All of the rift and postrift complexes include basaltoid fields in some places. As will be shown below, these rock complexes have specific isotope–geochemical parameters. The structure beneath the Tatar rift is characterized by drastic reduction of the continental crust (up to 25 km) and ascent of the asthenospheric layer up to the level of 50 km (Fig. 2). Therefore, this region is marked by high thermal flux (123–132 mW/m²). The temperature in the upper zone of the asthenospheric diapir is estimated at 1100°C [2–4]. The diapir is bounded by narrow gradient stages [4] that extend to higher lithospheric levels and generally correspond to strike-slip faults, which serve as boundaries of the Tatar and Japan basins. The faults presumably extend to the mantle and asthenosphere.

The *South Kuril basin* is also bounded by deep fault zones. This area incorporates the second (up to 20 km high) asthenospheric diapir (Fig. 2) accompanied by high thermal fluxes (346–354 mW/m²). High V values (8 km/s) in the overlying lithospheric mantle give way to anomalously low values (7.0–7.5 km/s) at the asthenosphere roof with the temperature increasing to 1200°C [1–3]. In the southwestern part of the basin, the Moho surface is located at a depth of 11–13 km; the continental crust is absent; and the Miocene marine-margin crust is only 7–10 km. Layer 3 of the marine-

^a Geological Institute, Russian Academy of Sciences, Pyzhevskii per. 7, Moscow, 119017 Russia; e-mail: filatova@ilran.ru

^b Geophysical Center, Russian Academy of Sciences, ul. Molodezhnaya 3, Moscow, 119991 Russia

margin crust (5–7 km) is composed of the basic–ultra-basic complex with $V = 6.4\text{--}7.2$ km/s [4, 7]. The overlying layers 1 and 2 ($V = 4.8\text{--}5.2$ km/s, thickness 2–2.8 km) are composed of folded and faulted, presumably Miocene, siliceous–terrigeneous and volcanic complexes. The undislocated late Miocene–Holocene cover (thickness up to 5 km, $V = 1.7\text{--}4.3$ km/s) consists of thin-bedded terrigenous (tuffaceous–terrigeneous in some places) rocks presumably deposited after the spreading [7]. Intense thermal fluxes and hydrothermal alterations probably fostered the consolidation and seismic transparency of the lower part of the sedimentary cover. The RWM seismic profile shows sectors with a thin-bedded structure, which is typical of the upper (seismic turbidite) section of the sedimentary cover. The continental crustal layer (~20 km thick) beneath the northeastern part of the South Kuril basin hosts the Geophysicist Seamount [7].

The Sikhote Alin and Sakhalin framing of the Tatar rift incorporates igneous rocks [8]. Their composition provides insights into deep zones of magma generation. Eocene–Oligocene (55–24 Ma) basaltoids of the initial rifting stage include calc-alkaline and alkaline rocks. Lower–middle Miocene volcanics (23–15 Ma) of the maximum extension stage are represented by tholeiites. Despite the presence of the Ta–Nb minimum, these rocks are compositionally close to the Pacific MORB (hereafter, P-MORB) variety. This fact is also evident from the $^{143}\text{Nd}/^{144}\text{Nd}$ – $^{87}\text{Sr}/^{86}\text{Sr}$ plot (Fig. 3). The Pb isotopic composition of these rocks is also confined to the P-MORB field (Fig. 3). The compositionally heterogeneous middle Miocene–Pliocene basaltoids [8] are dominated by OIB-type alkaline rocks, although they include rocks of the calc-alkaline type. These basaltoids are characterized by low $^{143}\text{Nd}/^{144}\text{Nd}$ values and a general trend oriented toward the EMI source. Data

points of terminal Miocene–Pliocene rocks, which are also assigned to this source, fall into the DUPAL mantle field in the $^{207}\text{Pb}/^{204}\text{Pb}$ – $^{206}\text{Pb}/^{204}\text{Pb}$ diagram (Fig. 3).

Dynamics of magmatism in the South Kuril basin can be reconstructed based on the study of volcanics from the Omu–Kamikawa and Monbetsu–Rubeshibe grabens [11], which extend in the meridional direction in the northeastern part of Hokkaido Island, the struc-

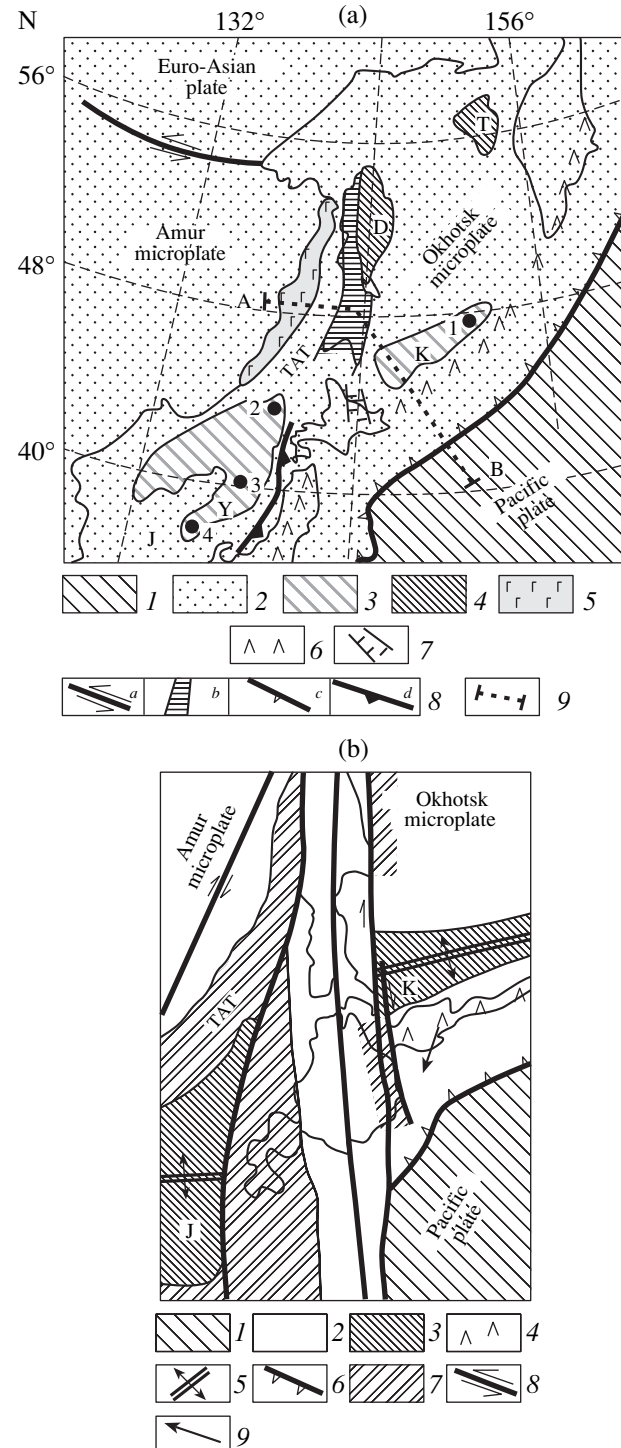


Fig. 1. (a) Present-day position of marginal basins in eastern Asia. (1) Oceanic crust; (2) continental crust; (3) basins related to continental-margin extension with marine-margin crust: (J) Sea of Japan, (Y) Yamato basin in the Sea of Japan, (K) South Kuril basin; (4) basins related to continental-margin extension with marine-margin and thin continental crust: (D) Deryugin, (T) Tinro; (5) Eocene–Pliocene volcanics of Sikhote Alin related to the Tatar continental rift (TAT); (6) Kuril volcanic arc; (7) system of Miocene grabens in northeastern Hokkaido Island; (8) plate boundaries: (a) transform, (b) diffuse transform, (c) convergent, (d) incipient convergent; (9) geotransverse profile. Numeral designations: (1) Geophysicist Seamount; (2–4) ODP holes in the Sea of Japan: (2) 795, (3) 794, (4) 797. (b) Position of the (J) Japan and (K) South Kuril marginal basins in the terminal early Miocene (20–16 Ma B.P.) during active spreading (modified after [3]). (1) Oceanic crust; (2) locally extended and thinned continental crust; (3) newly forming marine-margin crust; (4) retreating proto-Kuril island arc; (5) spreading zone; (6) subduction zone; (7) continental rifts: (TAT) Tatar; (8) strike-slip zones (arrows show the direction of horizontal displacement); (9) displacement direction of the proto-Kuril island arc during the formation of the South Kuril basin.

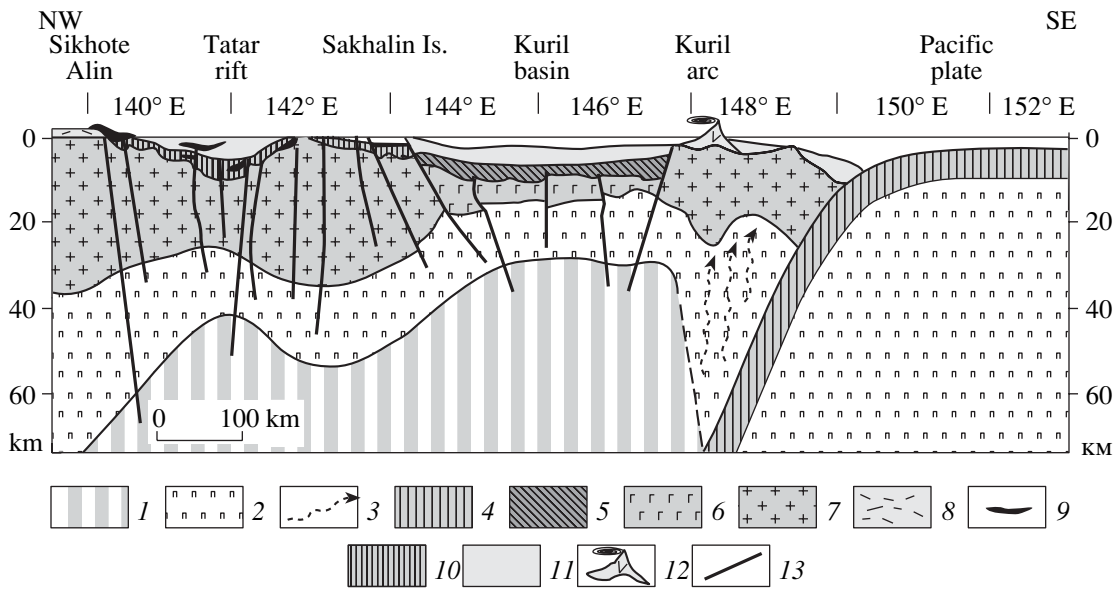


Fig. 2. Geotransverse of the Sea of Okhotsk region (modified after [1, 2]) (see AB in Fig. 1). (1) Asthenosphere; (2) upper mantle; (3) metasomatized (above the subduction zone) upper mantle; (4) oceanic crust of the Pacific plate; (5, 6) early–middle Miocene marine-margin crust of the South Kuril basin; (5) siliceous–terrigenous and volcanic complexes of layers 1 and 2 (undifferentiated), (6) basic–ultrabasic complexes of layer 3; (7) continental crust (including Mesozoic orogenic belts); (8) East Sikhote Alin continental-margin volcanoplutonic belt (Cretaceous–Paleocene); (9) Oligocene–Holocene (undifferentiated) magmatic complexes of extension zones represented by rifts and pull-apart basins (shown out of scale); (10) Eocene–middle Miocene terrigenous and volcanic–terrigenous complexes of the maximum extension stage in continental rifts; (11) upper Miocene–Holocene terrigenous complexes formed after rifting and spreading; (12) Kuril island arc; (13) strike-slip and normal faults.

ture of the northern marine sector (Fig. 1), and dextral strike-slip faults at the southwestern boundary of the South Kuril basin adjacent to the Sakhalin–Hokkaido zone. The graben-confined basaltoids include early–middle Miocene (14–11 Ma) varieties of the calc-alkaline type and middle–late Miocene (9–7 Ma) depleted basalts and andesites of the tholeiitic affinity. In terms of Sr and Nd isotopic ratios, the middle–late Miocene basalts and andesites are similar to early and middle Miocene rocks of the Tatar rift and marine-margin tholeiites of the Sea of Japan, i.e., rocks of the P-MORB type (Fig. 3). In terms of the Sr and Nd isotopic ratios, data points of the early–middle Miocene basaltoids of the calc-alkaline type make up two clusters. One cluster is nearly identical to the 9- to 7-Ma-old basalts, i.e., more similar to the P-MORB, whereas the second cluster is shifted toward the EMII field (Fig. 3). Both age groups of basaltoids from grabens of Hokkaido Island are related to different extension stages of the continental crust [11].

In the northeastern part of the South Kuril basin, eight basaltoid samples were dredged from the peak and slopes of the Geophysicist Seamount. The $^{40}\text{Ar}/^{36}\text{Ar}$ hornblende dating of two samples yielded 1.07 and 0.84 Ma [7]. Despite the general closeness to the calc-alkaline series, the basaltoids show significant variations in the contents of incoherent elements. Their isotopic heterogeneity is particularly prominent [7]. In terms of Sr and Nd isotopic ratios (Fig. 3), one rock group is very close to the P-MORB source, whereas the

second group shows stepwise reduction in the $^{143}\text{Nd}/^{144}\text{Nd}$ value and a trend toward the EMI source. These data suggest that the Geophysicist Seamount incorporates basaltoids probably related to various sources. This is also typical of rocks from Pacific islands.

The structure-controlled genesis of the Tatar and South Kuril basins should be considered in the general geodynamic setting of the terminal Paleocene. Under the influence of the Indo-Eurasian collision, the continental framing of the western Pacific, including the Amur and Sea of Okhotsk (hereafter, Okhotsk) microplates (Fig. 1), were disintegrated along submeridional dextral strike-slip fault zones. This process was responsible for the formation of transtension pull-apart basins characterized by maximum extension in the early–middle Miocene [4–6]. The united fault-restricted pull-apart structure, including the Japan and Tatar basins, evolved as continental-margin rift in the Eocene. In the first half of the Miocene, the Japan microcontinent was detached from Asia because of maximum extension, spreading of the Japan basin, and formation of the marine-margin crust (Fig. 1). The continental crust of the Tatar rift was reduced during this episode.

The South Kuril basin probably has a similar origin [3, 15]. Its opening was fostered by the southward migration of the Hokkaido and proto-Kuril island arc along the Sakhalin–Hokkaido dextral strike-slip zone (Fig. 1). Thus, although the South Kuril basin is nomi-

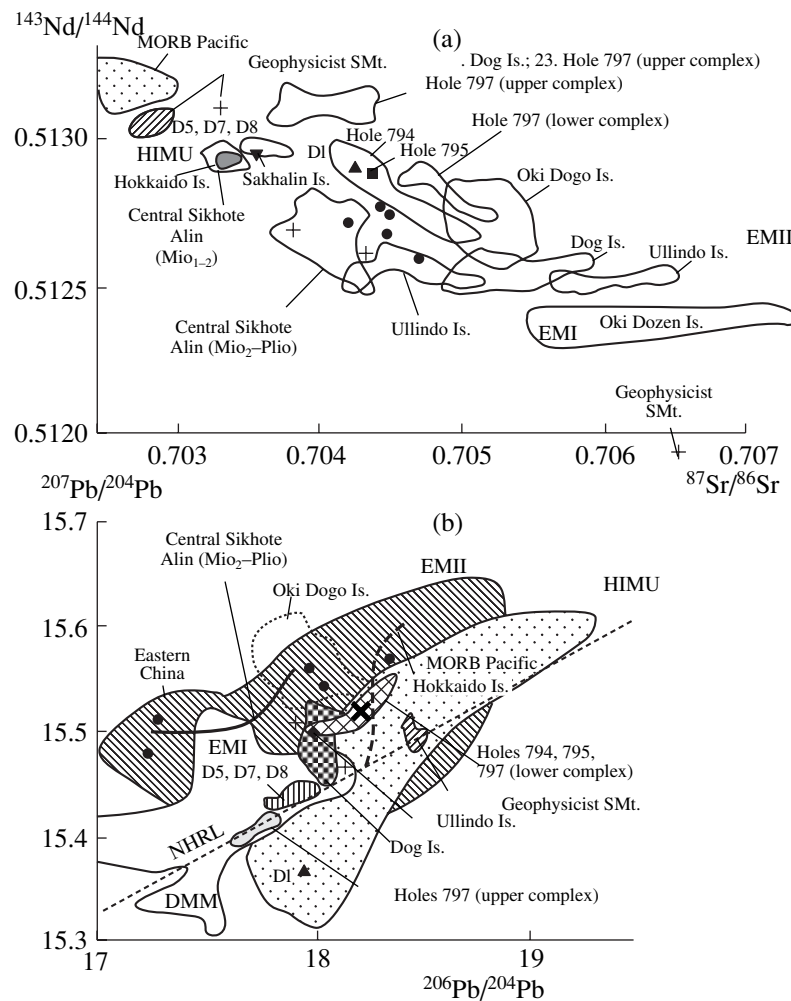


Fig. 3. (a) $^{143}\text{Nd}/^{144}\text{Nd}$ - $^{87}\text{Sr}/^{86}\text{Sr}$ and (b) $^{207}\text{Pb}/^{204}\text{Pb}$ - $^{206}\text{Pb}/^{204}\text{Pb}$ diagrams for Cenozoic basalts of extension zones at the eastern margin of Asia and in adjacent marginal basins [7–13 and references in 6, 9]. (a) Basalts of different ages. Early Miocene: holes drilled in the Sea of Japan—797 (lower complex), 794, 795; early–middle Miocene: Hole 797 (upper complex), dredging sites D1, D5, D7, and D8 (Yamato basin, Sea of Japan), Sakhalin Island, central Sikhote Alin; middle–late Miocene: grabens of Hokkaido Island; middle Miocene–Pliocene: central Sikhote Alin, southern Sikhote Alin (filled circles); Pliocene–Holocene: Geophysicist Seamount, South Kuril basin (oblique hatching and vertical crosses), Oki Dogo, Ullindo, Dog, and Oki Dozen islands (Sea of Japan). P-MORB, EMI, and EMII compositions are given after [14]. (b). Diamond designates early–middle Miocene basalts of central Sikhote Alin. Pacific MORB (P-MORB) and Indian MORB (I-MORB) compositions are given after [14]. (NHRL) Interface between I-MORB (DUPAL mantle) and P-MORB.

nally considered a back-arc in the present-day position, this basin is actually an analogue of the Japan pull-apart basin because of its genetic relation with strike-slip displacements within the continental crust, with the only difference being that the Japan basin bounded by two subparallel strike-slip fault systems has a diamond-shaped morphology. In contrast, the South Kuril basin has a triangular (in plan view) shape, because its opening was only governed by the western strike-slip zone and this process was terminated in the late Miocene. According to this model, the continental crust underwent maximum extension in the southwestern area of the basin adjacent to the major Sakhalin–Hokkaido strike-slip fault zone. In the early and initial late Miocene, precisely this area served as the spreading zone with the formation of a marine-margin crust. In

contrast, an extended continental crust was developed beneath the northeastern edge of the basin [7], although isotopic parameters of rocks of the Geophysicist Seamount suggest the possibility of diffuse spreading in this area as well.

The structural control of the genesis of extension zones discussed above indicates a passive mode of continental rifting in eastern Asia in the Cenozoic. The common style of structural control is emphasized by the similarity of geodynamic regimes during the formation of these structures, resulting in the common scenario of their evolution at different stages (initial rifting, maximum extension, and final episode related to changes in the character of interaction between lithospheric plates as a result of compression [6, 7]). Data on

the geotraverse (Fig. 2) indicate the presence of a correlation between extension intensity and structure at the crustal and subcrustal levels. Maximum extension in the study region (e.g., South Kuril basin) is related to rapture of the continental crust, formation of the marine-margin crust (spreading), asthenospheric upwelling to subsurface levels, and the consequent maximum thermal flux. The Tatar rift characterized by the thinning of the continental crust is also related to an asthenospheric diapir. However, the thermal flux here is less intense because of the significantly deeper location of the diapir (Fig. 2).

The similarity of dynamics of magmatism in extension zones correlates with the stagewise formation of basins and their deep structure. This fact makes it possible to reconstruct levels of magma formation and their variation in time. The available data on basins with various types of crust (Tatar and Japan basins) suggest that Eocene–Oligocene calc-alkaline basalts of the initial rifting stage are related to the reactivation of relict (Mesozoic) suprasubduction sources of the lithospheric mantle [6, 8]. The early–middle Miocene maximum extension (correspondingly, maximum asthenospheric upwelling) is represented by P-MORB tholeiites related to an asthenospheric source [6, 8]. Thus, magma sources varied from the upper mantle to the asthenospheric type during the evolution from the early rifting stage to the maximum extension stage. However, even marine-margin lavas of the maximum extension stage (e.g., rocks from the upper section of Well 797 and dredging sites D1, D5, D7, and D8 in the Sea of Japan), which represent the closest analogues of P-MORB rocks (Fig. 3), bear signs of hydrothermal alteration of rocks in the continental upper mantle (e.g., the presence of an amphibole–phlogopite assemblage). This type of mixing of isotope–geochemical signatures of basalts during the major stage of basin formation testifies to interaction between the dominant asthenospheric source and the metasomatized lithospheric mantle. The terminal Miocene–Holocene (postrift and postspreading) alkaline basalts, which are compositionally similar to OIB and EMI (EMII in some places) sources in terms of isotope–geochemical properties (Fig. 3), can genetically be related to the upper mantle material (according to model [6]), but the lithospheric source cannot be ruled out [8].

The asthenospheric upwelling fostered high thermal flux, magmatic activity, and heating of the sedimentary cover. These processes generated additional hydrocarbons and fluid flows that promoted the formation of petroleum deposits in sedimentary sequences of the Tatar rift.

CONCLUSIONS

The Japan–Tatar and South Kuril extension structures located along the Okhotsk geotraverse represent pull-apart basins related to strike-slip displacements. Their formation was mainly controlled by structural

factors related to interaction between lithospheric plates. Both structures emerged within a continental crust, although they differed in terms of the degree of extension: thinning of the continental crust or its fracturing (during spreading) and formation of the marine-margin crust. However, the Tatar and South Kuril basins show several similarities: synchronous evolution stages, similar dynamics of magmatism, and analogous structures of subcrustal zones. Both basins are characterized by asthenospheric upwelling related to lithospheric extension, and uplift of the asthenospheric diapir has a positive correlation with the degree of crustal extension. The latter factor was responsible for the following dynamics of magmatism: early stages of rifting were accompanied by the eruption of basalts related to the hydrothermally altered sectors of the upper mantle, whereas maximum extension correlated with tholeiites from asthenospheric sources.

ACKNOWLEDGMENTS

This work was supported by the Russian Foundation for Basic Research, project nos. 04-05-64025, 05-05-64917, 05-05-65198, and Nsh-748.2006.5.

REFERENCES

1. A. G. Rodnikov, L. P. Zabarinskaya, V. B. Piip, et al. *Vestn. KRAUNTS*, No. 5, 45 (2005).
2. *Structure and Dynamics of Lithosphere and Asthenosphere of the Sea of Okhotsk Region*, Ed. by A.G. Rodnikov, I.K. Tuezov, and V.V. Kharakhinov (Nats. Geofiz. Komitet, Moscow, 1996) [in Russian].
3. T. Takeuchi, *J. Geol. Soc. Jap.* **103**, 67 (1997).
4. *Explanatory Note to the Tectonic Map of the Sea of Okhotsk Region, Scale 1: 25 000 000*, Ed. by N.A. Bogdanov and V.E. Khain (ILOVM, Moscow, 2000) [in Russian].
5. L. Jolivet, J. P. Cadet, and F. Lalevee, *Tectonophysics* **149**, 89 (1988).
6. N. I. Filatova, *Geotectonics*, No. 6, 459 (2004) [*Geotektonika*, No. 6, 67 (2004)].
7. B. V. Baranov, R. Werner, K. A. Hoernle, et al., *Tectonophysics* **350**, 63 (2002).
8. S. Okamura, R. J. Arculus, and Yu. A. Martynov, *J. Petrol.* **46**, 221 (2005).
9. P. I. Fedorov and N. I. Filatova, *Geokhimiya*, No. 4, 3 (2002).
10. B. L. Cousens and J. F. Allan, *Proc. ODP. Sci. Res.* **127/128**, 805 (1992).
11. Y. Ikeda, R. J. Stern, H. Kagami, and Ch. H. Sun, *Island Arc* **9**, 161 (2000).
12. A. Pouclet and H. Bellon, *Proc. ODP. Sci. Lett.* **90**, 273 (1988).
13. M. Tatsumoto and Y. Makamura, *Geochim. Cosmochim. Acta* **55**, 3697 (1991).
14. S. R. Hart, *Earth Planet. Sci. Lett.* **90**, 273 (1988).
15. K. Kusunoki and G. Kimura, *Tectonics* **17**, 843 (1988).